Vacuum-Deposited Submonolayer Thin Films of a Three-Ring Bent-Core Compound

Yanhong Tang, Yan Wang, Guang Wang, Haibo Wang, Lixiang Wang, and Donghang Yan*

State Key Laboratory of Polymer Physics and Chemistry, Changchun Institute of Applied Chemistry, Chinese Academy of Sciences, Changchun 130022, People's Republic of China

Received: March 30, 2004; In Final Form: June 23, 2004

Submonolayer thin films of a three-ring bent-core (that is, banana-shaped) compound, *m*-bis(4-*n*-octyloxystyryl)-benzene (*m*-OSB), were prepared by the vacuum-deposition method, and their morphologies, structures, and phase behavior were investigated by atomic force microscopy (AFM) and transmission electron microscopy (TEM). The films have island shapes ranging from compact elliptic or circular patterns at low temperatures (below 40 °C) to branched patterns at high temperatures (above 60 °C). This shape evolution is contrary to the prediction based on the traditional diffusion-limited aggregation (DLA) theory. AFM observations revealed that two different mechanisms governed the film growth, in which the compact islands were formed via a dewetting-like behavior, while the branched islands diffusion-mediated. It is suggested *m*-OSB forms a two-dimensional liquid crystal at the low-temperature substrate that is responsible for the unusual formation of compact islands. All of the monolayer islands are unstable and apt to transform to slender bilayer crystals at room temperature. This phase transition results from the peculiar molecular shape and packing of the bent-core molecules and is interpreted as escaping from macroscopic net polarization by the formation of an antiferroelectric alignment.

1. Introduction

Recently, organic thin films have received growing interest because of their specifically notable electric and optical functions as active semiconducting layers. In the preparation of thin organic films, the vacuum-deposition method has been widely used due to its ability to control the growth of organic thin films with extremely high chemical purity and structural precision.[1] Up to now, the main interest was concentrated on films from conjugated materials, for example, polymers or oligomers derived from phenylene, phenylenevinylene, or thiophene.[2−4] Liquid crystals composed of calamitic molecules or discotic molecules began to draw attention from the areas of organic light-emitting devices, photovoltaics, and thin film transistors, etc., due to the high carrier mobilities, the anisotropic transport, and polarized emission resulting from the self-assembling properties and superamolecular structures (phases) of liquid crystals.[5,6] Banana-shaped liquid crystals (BLCs) as its new subfield have not yet been paid attention in such aspects, despite that much more attractive molecular self-organization and physical properties have been confirmed in BLCs.

The first discovery of ferroelectricity in nonchiral banana-shaped liquid crystals immediately attracted great interest of theoretical and technical viewpoints.[7−10] The molecules with a bent shape, also called "bent-core" liquid crystals, exhibit multiple possibilities for packing and thus have thermal polymorphism including the phases known from B1 to B7.[11] Unusual properties such as chirality and helical structures were found in some of the phases due to the spontaneous chiral and polar symmetry breaking.[12−15] A permanent dipole resulting from the two-dimensional electronic donor-π-acceptor structure appears along the two-fold symmetry axis; then ferro- or antiferroelectric properties relating to a macroscopic net polarization of the smectic layer can be expected.[12,16,17] Together with the second harmonic generation (SHG) activity shown by certain phases,[16,17] the bent-core compounds can be molecular functional materials and have a potentially promising application in various kinds of organic devices besides in liquid crystal displays. Usually, organic functional materials have been processed as films serving as active layers in devices; thereby the studies on growth mechanism, molecular ordering, and the overall film morphology are of prime importance for device design. As far as the bent-core compounds are concerned, although a considerable effort has been devoted to recognize the bulk liquid crystals, their film form has scarcely been investigated.[18]

Recently, we initiated the investigation of the vacuum-deposited films of banana-shaped compounds on the morphology and molecular orientations, which are of great value for future technical applications. On the other hand, despite a great deal of endeavor, the relationships between the molecular structure and the physical properties of the BLCs are not well established. For such studies, the film techniques provide powerful methods in understanding the particular properties on the molecular scale.[12]

Our interest is a three-ring bent-core compound *m*-bis(4-*n*-octyloxystyryl)benzene (*m*-OSB, Figure 1). In contrast with the conventional five-ring system[11] containing sensitive Schiff-base units, *m*-OSB has a simple chemical structure and a good thermal stability up to 276 °C (indicated by thermogravimetric analysis) and can be processed as pure thin films in high vacuum conditions. Thus, it should be a good model compound for studying the film physics of the bent-core species. In this work, *m*-OSB films were grown on mica at varied substrate temperatures and submonolayer coverages. Interesting island shape evolution and phase transition related to the particular molecular configuration were observed in this system.

2. Experimental Section

The compound *m*-OSB was synthesized by reacting 4-octyloxybenzaldehyde with 1,3-xylylene tetrabutyldiphosphonate

* To whom correspondence should be addressed. E-mail: yandh@ciac.jl.cn.

10.1021/jp048607f CCC: $27.50
Published on Web 07/31/2004

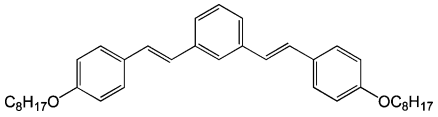

Figure 1. Chemical structure of *m*-OSB.

using the G. Wittig reaction, and the bulk properties were characterized by differential scanning calorimetry, polarizing light microscopy, powder X-ray diffraction, and electronic diffraction. The bulk crystal belongs to the orthorhombic $P2_12_12_1$ space group with cell parameters of $a = 0.74$ nm, $b = 0.63$ nm, and $c = 7.21$ nm. The molecules are aligned as a layered structure. In the unit cell, the molecular long axes are parallel to the *c*-axis and the bending direction of the molecules between neighboring layers is opposite, leading to the so-called antiferroelectric arrangement.[12] In addition, a highly ordered smectic liquid crystalline phase or a second crystal phase was found between 66 and 155 °C, and above 155 °C it is an isotropic liquid. The phase identification as well as detailed experimental results will be reported in a forthcoming paper.

m-OSB thin films were grown by vacuum evaporation on freshly cleaved mica under a pressure of 2×10^{-3} Pa. The substrate temperatures were varied from room temperature (RT, 25 ± 2 °C) up to 140 °C, referring to the bulk phase sequence. During the vacuum deposition, the source temperature was held at ~176 °C and the amount of the deposited sample was controlled in a submonolayer range. The sample was extracted from the chamber quenched to room temperature when the desired amount had been deposited. The film morphology was recorded using a nanoscope IIIa atomic force microscope (AFM: Digital Instruments, Santa Barhara, CA) in tapping mode. Electron diffractions were performed using a JEOL (2000 EX I) electron microscope with the sample evaporated on carbon films supported by mica, and then the films were transferred onto Cu grids for the diffraction measurements.

3. Results and Discussion

3.1. Thin Film Morphology with Substrate Temperature. The AFM topographies of *m*-OSB submonolayers are shown in Figure 2, and distinct features are observed in the island morphology as a function of substrate temperature. The film deposited at RT is composed of compact elliptic droplet-like islands (Figure 2a). Analogous islands can be found to form at the substrate temperatures from 0 to 40 °C (occasionally circular droplet-like islands are formed at 40 °C as shown in Figure 2b), indicating the same mechanism governs the film growth in this temperature range. Figure 2c shows the film islands deposited at 60 °C. A significant morphology transition to branched growth is observed. At a still higher substrate temperature of 120 °C (Figure 2d), the islands are even more ramified and side-branching occurs on each arm, similar to dendritic growth. Both the length and the width of the branches increase with increasing substrate temperature.

Recently, much work has been done to investigate two-dimensional (2D) island shape evolution with substrate temperature in metal-on-metal epitaxy.[19−22] Typically, the island formed at low temperatures has a fractal pattern, then has dendritic growth at elevated temperatures, and finally tends to be compact at high temperatures, in agreement with predictions based on the classic diffusion-limited aggregation (DLA) model[23] taking into account edge diffusion in real growth. It is suggested that the adatoms deposited from the vapor phase randomly diffuse on the surface until they reach the perimeter of a growing island. If the adatoms stick to the island upon

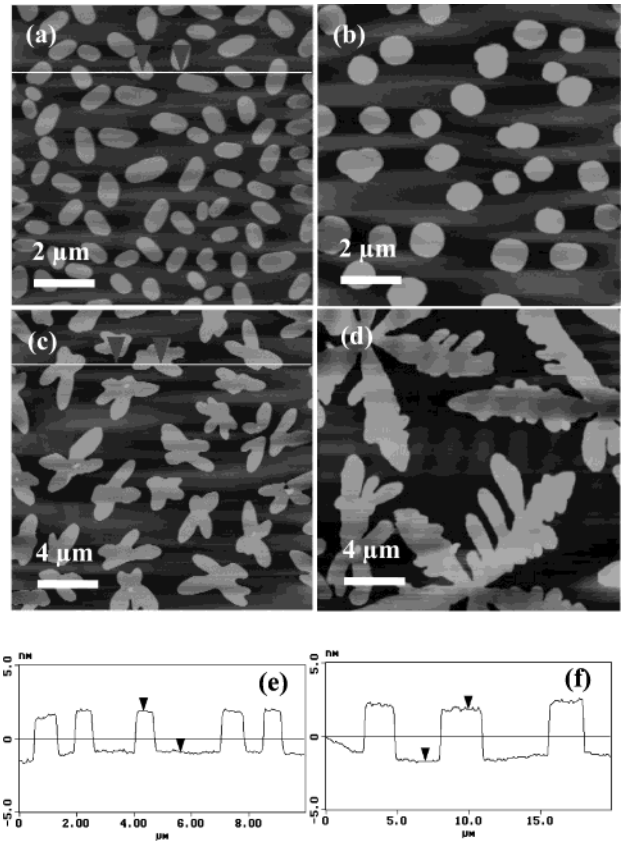

Figure 2. AFM images for the m-OSB monolayer islands deposited on mica at substrate temperatures of (a) RT, (b) 40 °C, (c) 60 °C, and (d) 120 °C. Cross-sections through the droplet islands of (a) and branched islands of (c) are shown in (e) and (f), respectively.

hitting, then standard DLA growth is formed. In fact, they are not fixed but attempt to relax locally to find an energetically more favorable configuration. Sufficiently relaxing along the island edges will lead to a compact island; otherwise a fractal-like island will be formed. Increasing substrate temperature will increase the degree of local relaxation and favor the transition from a fractal to a compact island.[19−22,24] The same mechanism as developed for inorganic homo- and heteroepitaxy could be operative in organic 2D systems.[25] The evolution, however, appears to be reversed in the case of *m*-OSB submonolayer islands. Compact *m*-OSB islands are formed at lower temperatures, and fractal-like *m*-OSB islands are formed at higher temperatures. A similar phenomenon has recently been reported in surfacant-mediated inorganic expitaxy, which was attributed to reaction-limited aggregation.[26−28] In this work, the high density of the compact island indicates a short diffusion length of the migrating molecules on the substrate surface in comparison with the branched islands, and the formation of the *m*-OSB compact islands is therefore not attributed to sufficient relaxation of adsorbed molecules along the island edges. Annealing the two types of islands at 140 °C, one can find the compact droplet-like islands are unchanged, giving a thermodynamic equilibrium shape, while the branched islands show the trend to be more compact. We resolved these problems experimentally and theoretically.

Repeated experiments have been carried out to confirm the island morphologies. The branched islands could be found in every case, but the films grown at the substrate temperatures below 40 °C were not always composed of complete droplets; sometimes they coexisted with disordered film. Moreover, the apparent height of the droplet islands depended, to a certain

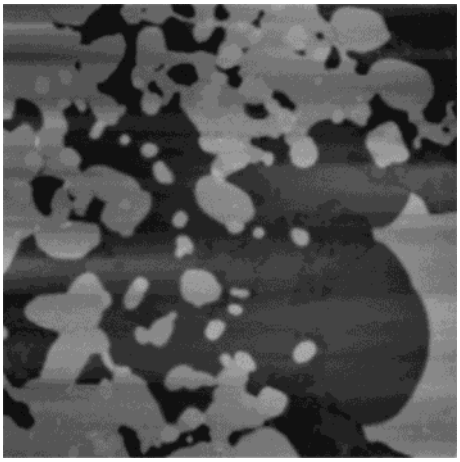

Figure 3. A 4 × 4 μm^2 AFM image shows a complex morphology consisting of droplet-like islands and disordered film fabricated at room temperature.

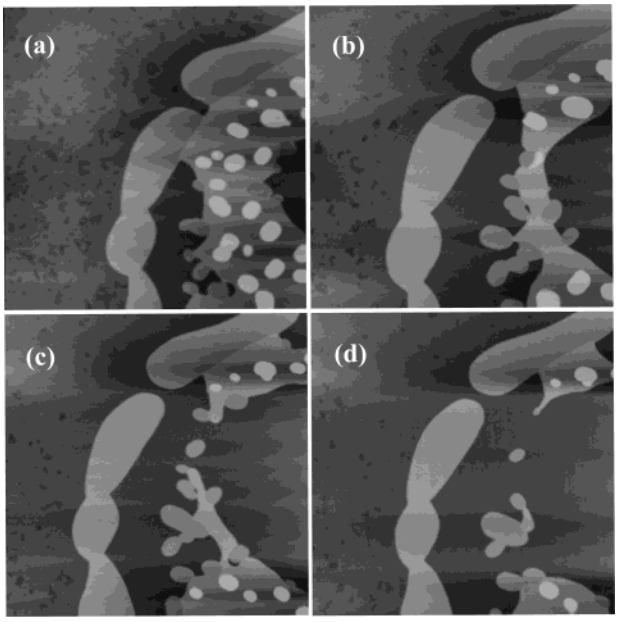

Figure 4. Time evolution of droplet islands and disordered film: (a) $t = 0$ min; (b) $t = 50$ min; (c) $t = 80$ min; (d) $t = 100$ min. Note that the time original is arbitrary. One can see in views (b), (c), and (d) that the points with high curvature retract. The size of the images is 4 × 4 μm^2.

extent, on the scan direction and the set point value if the contact mode was adopted for imaging. The branched islands were not so influenced by these parameters. It seems that the droplet-like islands are softer than the branched islands. To eliminate the influence, the tapping mode was used for the AFM imaging. High-quality topographies can be obtained, but disordered films can still be observed in some cases for the fabrication of droplet islands, and a typical topographical image is shown in Figure 3, which displays a complex morphology consisting of both the droplet-like islands and the disordered film. Usually, we imaged the films in 2 or 3 h after vacuum deposition. Maybe some important information has been neglected as a result of the delayed scanning? We then tried to conduct the AFM imaging after deposition as soon as possible and to explore the relation between the droplet islands and disordered films. Figure 4 shows four snapshots, revealing a morphology evolution with time. Although we cannot extract a very precise mechanism from these images, it permits us to deduce that the droplets were not formed as they grew but transformed from a disordered film via a dewetting-like process after deposition. We assume that the *m*-OSB vapor molecules are immediately "frozen" when the substrate surface is first impinged, leading to a disordered and featureless film. The disordered film is unstable due to the high surface free energy and will relax to an energetically favorable state. The formation of droplet islands is a spontaneous process, because from the viewpoint of thermodynamics, the surface tends to minimize the free energy by reducing the surface area. Islands with an elliptic or circular shape are approved to have a minimum of boundary free energy form from the disordered film. In addition, the bent-core molecules are strongly dipolar, and the strong cohesion resulting from the long-range dipolar forces helps hold the molecules together. During this transformation, the film displays a liquidlike behavior that the points with high curvature retract, while the defined boundaries between droplets informs us that the droplet island may be in a liquid crystal phase.

Nevertheless, the formation of the branched island is relatively simple and can be understood by a diffusion-controlled growth theory. The irregularly structured perimeter of these islands is reminiscent of dendritic growth. In this growth regime, edge diffusion plays an important role. That is, based on the "hit-and-stick" model of standard DLA fractal growth, the molecules diffuse on the surface and simultaneously along the island edge, but the rate at which it finds a stable anchoring site at island edges is lower than that of the molecule diffusing to the island, thereby yielding a fractal-like island with wide thickness. The diffusional distance of molecules increases with the temperature, leading to a decrease in island density and accordingly an increase in island size, as demonstrated by comparing the *m*-OSB branched islands in Figure 2c and d. Further increase of the substrate temperature will drive the dendritic growth into compact growth.[20−22] Because a nonnegligible desorption of *m*-OSB molecules occurs above 150 °C, more compact islands cannot be realized in this system. As mentioned at an early section, a long-time annealing at 140 °C of the branched *m*-OSB islands will drive them more compact. These results support the diffusion-controlled growth mechanism for the branched islands.

Diffusion-mediated growth can be treated in the framework of the rate equation theory.[29−32] The island density contains direct information about molecule diffusion and should show Arrhenius behavior upon variation of the substrate temperature.[32−34] Quantitative analysis has been carried out for the branched islands derived from five thin films prepared in the temperature range from 60 to 140 °C. As the deposition time and deposition rate were constant for all of the films, the average island area is used here to substitute the island density for the plot. The calculation method of the island area was described in previous literature[35] with NIH-IMAGE software. For each substrate temperature, 30−50 islands were chosen from different regions of the sample for the averaging. Figure 5 shows the logarithm of the average area versus inverse temperature, exhibiting a clear Arrhenius-type behavior. The activation energy can then be estimated from the fitting to be 0.42 eV, more than the thermal energy (RT = 0.036 eV) supplied by 140 °C substrate, suggesting a noncompact island growth in the experiment temperature range.

Different from the regular dendritic structure, which anisotropically ramifies with branching along some preferred directions at crystal substrates,[19−22,24] the branches of the *m*-OSB islands show no simple correlation with the symmetry axes of the mica substrate, indicating that the substrate has a minor effect on the film morphology and there is a stronger interaction

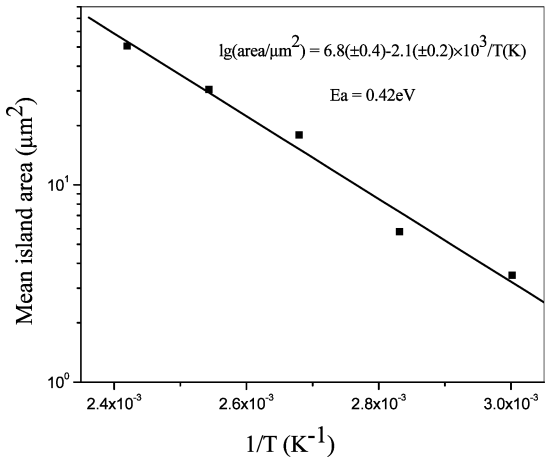

Figure 5. Plot of the average island area versus inverse temperature, which demonstrates a clear Arrhenius-type behavior.

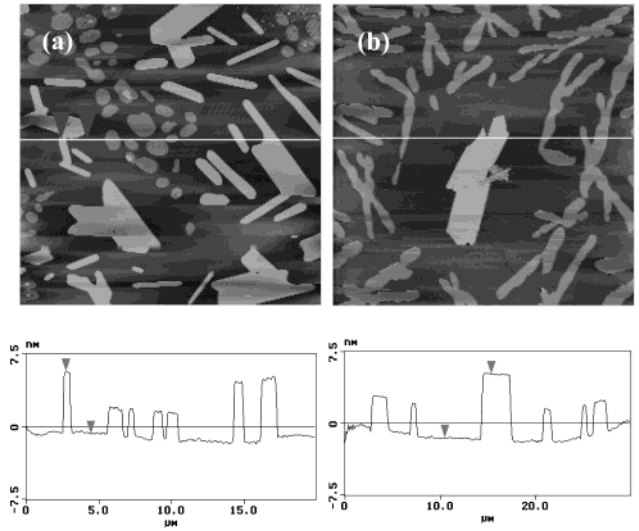

Figure 6. AFM images demonstrate the phase transition from the monolayer of (a) droplet islands and (b) branched islands to slender bilayer crystals. The cross-sectional profile below the image was measured across the line marked in it.

between the adsorbed molecules than that between the molecules and the substrate, as expected from sterically induced tight packing of the bent-core molecules.[11] We checked this by varying the substrate using carbon film and silicon oxide, and the essential features of the island shape were reproduced satisfactorily. Cross-sectional analyses (see Figure 2e and f) have been conducted on different islands from several samples, giving a mean height of 2.5 ± 0.3 nm for the droplet islands, and 2.8 ± 0.3 nm for the branched islands, both smaller than the length of a *m*-OSB molecule in an all-trans conformation (∼3.6 nm).[36] This suggests that, in monolayer films, the *m*-OSB molecules stand tilted on the substrate surface, so that the balance between the aggregates and the substrate can be maintained.

In views of the above investigations, the counterintuitive compact-to-fractal island shape transition with increased temperature is ascribed to the phase change between 40 and 60 °C (this can be corroborated by electron diffraction patterns shown in Figure 7a and b and will be discussed subsequently), and two extraordinarily differed mechanisms govern their growth, respectively. The formation of the *m*-OSB compact islands is via a dewetting-like behavior, which has never been reported in vacuum-deposited films. We surmise such a phenomenon is related to the molecular configuration because molecules of this shape have a tendency to form liquid crystals. Even though the

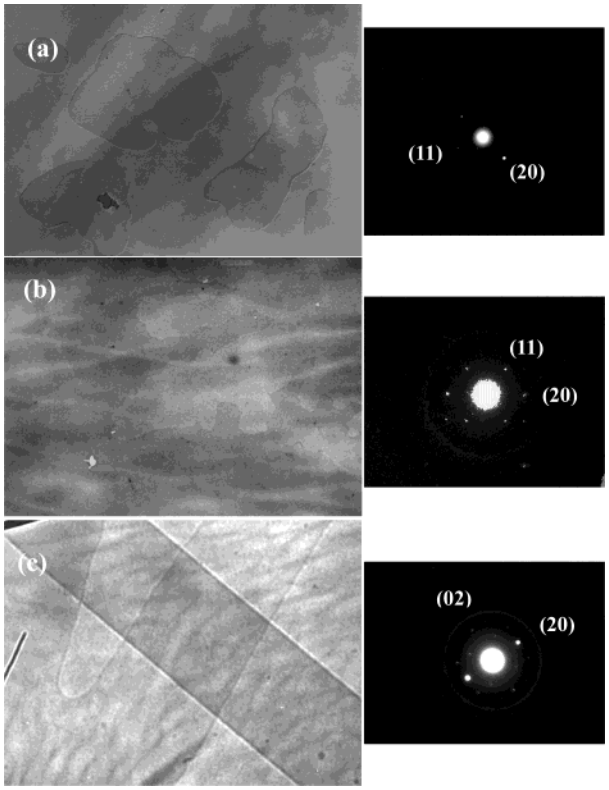

Figure 7. Electron diffraction patterns and corresponding micrographs of *m*-OSB films containing (a) droplet islands, (b) branched islands, and (c) slender islands.

m-OSB molecule under investigation has not been confirmed as liquid crystalline, in the present case, it is possible that the island and film below 40 °C are in two-dimensional liquid crystal phases. The spontaneous formation of elliptic or circular islands from as-deposited film is reminiscent of water droplets formed from water film on a nonwetting surface, what we call "dewetting". During this process, the *m*-OSB islands and film display a liquidlike act of shrinking, while the flat surface of the droplet-like islands and the defined grain boundaries between the coalescent islands mean the *m*-OSB molecules in them are in an ordered alignment. Because of the fluid property, the growth of the compact islands is not dominated by kinetic origin, unlike the island grown at above 60 °C, which is a solid thin film and formed by *m*-OSB molecular self-diffusion.

3.2. Phase Behavior of Monolayer Films. In addition to the interesting island shape evolution, the films exhibit even more interesting phase behavior. After being stored at room temperature for a few days, the films will change greatly in morphology. The monolayer islands, regardless of whether they are of compact or branched patterns and regardless of what the substrate is, will transform to a new type of grain, typically presented as in Figure 6. Figure 6a shows the scenario that the droplet islands formed at 40 °C are undergoing another morphological transition to extended lamellar crystals, and Figure 6b shows the same transition from 120 °C-deposited branched islands. The height of the new islands, which we generally call "slender islands" below, is 6.6−7.2 nm, corresponding to twice the molecular length. Bilayer films with the molecular long axis perpendicular to the substrate surface are consequently proposed for the slender islands. Why are monolayer films, whatever the morphology or microstructure, unstable and finally transform to bilayer islands? To explore the origin of this transition, it is necessary to understand the microscopic

TABLE 1: The Calculated Lattice Parameters for the Three Types of Islands

island	droplet	branched	slender
a (nm)	0.76	0.74	0.74
b (nm)	0.65	0.63	0.63

organization of the film islands before and after the transition. Electron diffraction was used to investigate these films.

Figure 7 shows the typical electron diffraction (ED) patterns and corresponding transmission electron micrographs of *m*-OSB films on amorphous carbon substrates. The film grown at room temperature consists of compact islands with an irregular boundary, which are caused by the rough surface of carbon film relative to mica (Figure 7a). In its diffraction pattern, the spots are much sparser than those of the branched island (Figure 7b) and the slender island (Figure 7c), revealing a lower degree of order. The branched islands have a long-range crystalline order indicated by the clear and regular diffraction spots in the pattern of Figure 7b. The diffraction pattern shown by the slender island is very similar to that of the *m*-OSB bulk crystal, whose sharply defined diffraction peaks indicate that the slender lamella is a perfect single crystal (see Figure 7c). All three patterns present a rectangular lattice, and their planar lattice constants are listed in Table 1. From the constants and the aforementioned AFM measurements, we know that the slender crystalline island has the same lattice structure and vertical molecular orientations as the bulk crystal despite that there are only two layer molecules in the former. For the monolayer films, each branched island forms a two-dimensional single crystal with the lattice spacings (*a* and *b*) also similar to those of the bulk crystal except that the molecules in the film case are tilted with respect to the (*ab*) plane, the substrate surface. The droplet island has a shorter-range positional order and slightly larger lattice parameters than does the branched island, suggesting a nondense molecular packing that induces a more pronounced tilt of the molecules, indicated by the AFM-measured island-height difference between the droplet island and the branched island.

Now, according to the film structures and the bent-core shape of the molecule, we can explain this phase transition. In the monolayer film, the *m*-OSB molecules adopt the characteristic layer packing of banana-shaped molecules in which their bent direction is uniformly aligned within the layer (schemed as in Figure 8a), giving rise to a macroscopic polar order.[7,12,16,17] In this sense, the film is ferroelectic. Investigations on bent-core liquid crystals reveal that usually the antiferroelectric phases represent the ground states, whereas the ferroelectric states can only be achieved after applying a sufficiently strong external electric field. They are not stable and relax back to the antiferroelectric state after the electric field is switched off.[37] Here, we can say that the ferroelectric film is unstable and the system tends to escape from the resulting macroscopic net polarization. Thus, the molecules in the monolayers are apt to reorganize as bilayers with the bending direction in the adjacent layers antiparallel, which has been confirmed as an antiferroelectric alignment in the bulk crystal. At the same time, the molecules change their orientation from tilted to upright with respect to the substrate (Figure 8b). In this way, the dipoles cancel out between layers and the system can eliminate the macroscopic polarization. During the course of study on the banana-shaped liquid crystals, Watanaba et al.[38,39] proposed several possible structures to escape from the macroscopic polarization: frustrated structure, helical structure, and antiferroelectric structure. This work presents direct evidence for the spontaneous formation of an antiferroelectric structure in nonchiral banana-shaped liquid crystals.

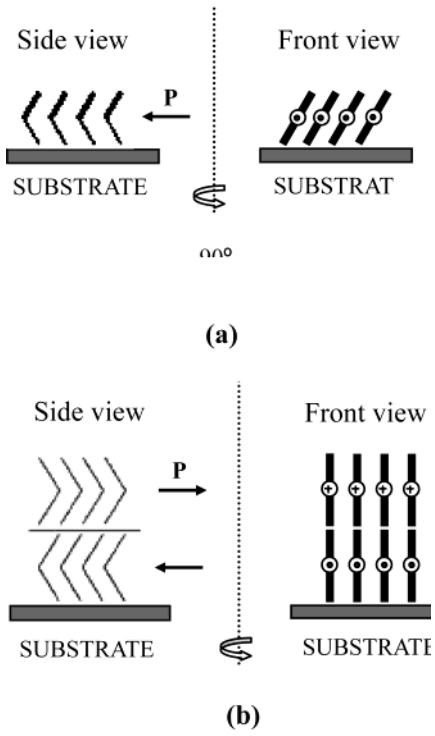

Figure 8. Schematic representations of molecular arrangements in the following: (a) monolayer of droplet island or branched island (the molecules are tilted relative to the normal of the substrate, and a macroscopic polar order is formed); and (b) bilayer of slender crystal with perpendicular orientation of the molecules and opposite alignment of the bent directivity between the layers. Thus, the system eliminates the macroscopic polarization (P: polarization).

It is noted that, maybe due to their liquid crystal nature, the droplet islands are even more unstable than the branched islands at room temperature, so within a comparable time the former have a faster phase transition.

4. Conclusions

We have investigated the morphology, structure, and phase behavior of vapor-deposited submonolayer thin films of a three-ring bent-core compound *m*-OSB. The structure and growth of the submonolayer are determined by the properties of the constituent molecules, their intermolecular interactions, the substrate structure, and the substrate−adsorbate interactions. In our case, the two later factors are found to be less important. The bent-core molecules are strongly dipolar, and aggregates made of such molecules are destined to have strong intermolecular interactions. Furthermore, a polar layer alignment is preferred to this class due to the sterically induced packing of the bent cores. As a consequence, specific island morphologies and phase behavior different from those of films made of other organic molecules, for example, linear molecules, may be anticipated.[40] An abnormal evolution of island shapes versus deposition temperature was observed in this system in terms of traditional DLA theory. We attribute it to the finding that *m*-OSB forms a 2D liquid crystalline phase at temperatures below 40 °C. Because a rapid nucleation takes place at low temperatures, condensation results in a disordered film with high surface energy. The dipolar cohesion between *m*-OSB molecules and the strong tendency to minimize the surface free energy drive the spontaneous formation of droplet-like islands with elliptic or circular shape shortly after deposition. The fluidlike behavior demonstrated during the transition and the short-range positional order of the molecules in the droplet islands (the orientational

order is indicated by the molecular self-assembly in the monolayer) are modestly indicative of a liquid crystal phase, although it was predicted that bent-core compounds with three aromatic rings are unfavorable for the formation of liquid crystals.[41,42] At elevated temperatures above 60 °C, the adsorbed molecules are activated by thermal energy supplied by the substrate. The growth of the branched island is controlled by molecular diffusion and hence can be understood in the framework of conventional nucleation theory for vacuum vapor deposition. As the temperature increases, the mobility of the molecules enhances, and the molecules have a longer time to diffuse, aggregate, and relax, leading to a large fractal-like island and a crystalline ordered alignment. A more distinct effect of the special molecular shape and packing of the bent-core molecules on the submonolayer films is the phase transition from monolayer to bilayer. Because a macroscopic polar order is easily formed in a monolayer, the system is unstable. An antiferroelectic bilayer structure was then formed to cancel out the spontaneous polarization. Thus, the novel phenomenon of a nonchiral molecule forming an antiferroelectic phase has been verified directly and simply by the film technique.

Acknowledgment. This work was financially supported by the Special Funds for Major State Basic Research Projects (2002CB613400) and the National Natural Science Foundation of China (90301008, 20025413).

References and Notes

(1) Forrest, S. R. *Chem. Rev.* **1997**, *97*, 1793.
(2) Gundlach, D. J.; Lin, Y. Y.; Jackson, T. N.; Schlon, D. G. *Appl. Phys. Lett.* **1997**, *71*, 3853.
(3) Garnier, F.; Yassar, A.; Hajlaoui, R.; Horowitz, G.; Deloffre, F.; Servet, B.; Ries, S.; Alnot, P. *J. Am. Chem. Soc.* **1993**, *115*, 8716.
(4) Borroughes, J. H.; Bradley, D. D. C.; Brown, A. R.; Marks, R. N.; Friend, R. H.; Burn, P. L.; Holmes, A. B. *Nature* **1990**, *347*, 539.
(5) O'neill, M.; Kelly, S. M. *Adv. Mater.* **2003**, *13*, 1135 and references therein.
(6) Grell, M.; Bradley, D. D. C. *Adv. Mater.* **1999**, *11*, 895 and references therein.
(7) Niori, T.; Sekine, F.; Watanabe, J.; Furukawa, T.; Takezoe, H. *J. Mater. Chem.* **1996**, *6*, 1231.
(8) Niori, T.; Sekine, F.; Watanabe, J.; Furukawa, T.; Takeoza, H. *Mol. Cryst. Liq. Cryst.* **1997**, *301*, 337.
(9) Sekine, F.; Takanashi, Y.; Niori, T.; Watanabe, J.; Takeoza, H. *Jpn. J. Appl. Phys.* **1997**, *36*, L1201.
(10) Sekine, F.; Niori, T.; Watanabe, J.; Furukawa, T.; Choi, S. W.; Takeoza, H. *J. Mater. Chem.* **1997**, *7*, 1307.
(11) Pelzl, G.; Diele, S.; Weissflog, W. *Adv. Mater.* **1999**, *11*, 707 and references therein.
(12) Link, D. R.; Natale, G.; Shao, R.; Maclennan, J. E.; Clark, N. A.; Körblova, E.; Walba, D. M. *Science* **1997**, *278*, 1924.
(13) Sekine, T.; Noiri, T.; Sone, M.; Watanabe, J.; Choi, S. W.; Takanishi, Y.; Takazoe, H. *Jpn. J. Appl. Phys.* **1997**, *36*, 6455.
(14) Thisayuka, J.; Nakayama, Y.; Kawauchi, S.; Takezoe, H.; Watanabe, J. *J. Am. Chem. Soc.* **2000**, *122*, 7441.
(15) Thisayukta, J.; Kawauchi, S.; Takezoe, H.; Watanabe, J. *Jpn. J. Appl. Phys.* **2001**, *40*, 3277.
(16) Macdonald, R.; Kentischer, F.; Warnick, P.; Heppke, G. *Phys. Rev. Lett.* **1998**, *80*, 4408.
(17) Shoi, S. W.; Kinoshita, Y.; Takezoe, H.; Niori, T.; Watanabe, J. *J. Jpn. Appl. Phys.* **1998**, *37*, 3408.
(18) Kinoshita, Y.; Park, B.; Takezoe, H.; Niori, T.; Watanabe, J. *Langmuir* **1998**, *14*, 6256.
(19) Michely, T.; Hohage, M.; Bott, M.; Comsa, G. *Phys. Rev. Lett.* **1993**, *70*, 3943.
(20) Zhang, Z. Y.; Chen, X.; Lagally, M. G. *Phys. Rev. Lett.* **1994**, *73*, 1829.
(21) Bales, C. S.; Chrzan, D. C. *Phys. Rev. B* **1994**, *50*, 6057.
(22) Bales, C. S.; Chrzan, D. C. *Phys. Rev. Lett.* **1995**, *74*, 4879.
(23) Written, T. A.; Sander, L. M. *Phys. Rev. Lett.* **1981**, *47*, 1400.
(24) Zhang, Z. Y.; Lagally, M. G. *Science* **1997**, *276*, 377.
(25) Heringdorf, F. M. z.; Reuter, M. C.; Tromp, R. M. *Nature* **2001**, *412*, 517.
(26) Liu, B. G.; Wu, J.; Wang, E. G.; Zhang, Z. Y. *Phys. Rev. Lett.* **1999**, *83*, 1195.
(27) Wu, J.; Liu, B. G.; Zhang, Z. Y.; Wang, E. G. *Phys. Rev. B* **2000**, *61*, 13212.
(28) Chang, T. C.; Hwang, I. S.; Tsong, T. T. *Phys. Rev. Lett.* **1999**, *83*, 1191.
(29) Stowell, M. J.; Hutchinson, T. E. *Thin Solid Films* **1971**, *8*, 41.
(30) Stowell, B. M. *Philos. Mag.* **1972**, *26*, 361.
(31) Robins, J. L. *Appl. Surf. Sci.* **1988**, *33/34*, 379.
(32) Venables, J. A.; Spiller, G. D. T.; Hanbücken, M. *Rep. Prog. Phys.* **1984**, *47*, 399.
(33) Brune, H.; Röder, H.; Boragon, C.; Kern, K. *Phys. Rev. Lett.* **1994**, *73*, 1955.
(34) Bott, M.; Hohoge, M.; Morgenstern, M.; Michely, T.; Comsa, G. *Phys. Rev. Lett.* **1996**, *76*, 1304.
(35) Biscarini, F.; Zamboni, R.; Samori, P.; Ostoja, P.; Taliani, C. *Phys. Rev. B* **1995**, *52*, 14868.
(36) The extended length of *m*-OSB was calculated by molecular modeling using MOPAC/AM1 for the most stable conformation.
(37) Walba, D. M.; Korblova, E.; Shao, R. F.; Maclenna, J. E.; Link, D. R.; Glaser, M. A.; Clark, N. A. *Science* **2000**, *288*, 2181.
(38) Watanaba, J.; Nakata, Y.; Simizu, K. *J. Phys. II (France)* **1994**, *4*, 581.
(39) Watanaba, J.; Niori, T.; Sekine, T.; Tekezoe, H. *Jpn. J. Appl. Phys.* **1998**, *37*, L139.
(40) For comparison, a series of submonolayer films from a linear compound *p*-bis(4-*n*-octyloxystyryl)benzene were prepared by vacuum deposition on mica at different substrate temperatures. Oval compact islands were found to form at room temperature. As the temperature increased, the island shape developed as quasi-hexagon. Such an evolution can be understood by conventional diffusion-controlled theory.
(41) Vill, V. *Landolt-Börsteint Numerical Data and Functional Relationship in Science and Technology*; Springer: Berlin, 1992−1998; Vol. 7a−f.
(42) Coden, M.; Hayashi, S.; Nishimura, K.; Kusabayashi, S.; Takenaka, S. *Mol. Cryst. Liq. Cryst.* **1984**, *106*, 31.